Langmuir

Article

pubs.acs.org/Langmuir

Assembly of Poly(dopamine)/Poly(*N*-isopropylacrylamide) Mixed Films and Their Temperature-Dependent Interaction with Proteins, Liposomes, and Cells

Yan Zhang,[†,‡] Karthiga Panneerselvam,[‡] Ryosuke Ogaki,[‡] Leticia Hosta-Rigau,[‡] Rebecca van der Westen,[‡] Bettina E. B. Jensen,[§] Boon M. Teo,[‡] Meifang Zhu,*[,†] and Brigitte Städler*[,‡]

[†]State Key Laboratory for Modification of Chemical Fibers and Polymer Materials, College of Material Science and Engineering, Donghua University, Shanghai 201620, People's Republic of China

[‡]iNANO, Aarhus University, Gustav Wieds Vej 14, DK-8000 Aarhus, Denmark

[§]Department of Chemistry, Aarhus University, Langelandsgade 140, DK-8000 Aarhus, Denmark

Supporting Information

ABSTRACT: Many biomedical applications benefit from responsive polymer coatings. The properties of poly(dopamine) (PDA) films can be affected by codepositing dopamine (DA) with the temperature-responsive polymer poly(*N*-isopropylacrylamide) (pNiPAAm). We characterize the film assembly at 24 and 39 °C using DA and aminated or carboxylated pNiPAAm by a quartz crystal microbalance with dissipation monitoring (QCM-D), X-ray photoelectron spectroscopy, UV−vis, ellipsometry, and atomic force microscopy. It was found that pNiPAAm with both types of end groups are incorporated into the films. We then identified a temperature-dependent adsorption behavior of proteins and liposomes to these PDA and pNiPAAm containing coatings by QCM-D and optical microscopy. Finally, a difference in myoblast cell response was found when these cells were allowed to adhere to these coatings. Taken together, these fundamental findings considerably broaden the potential biomedical applications of PDA films due to the added temperature responsiveness.

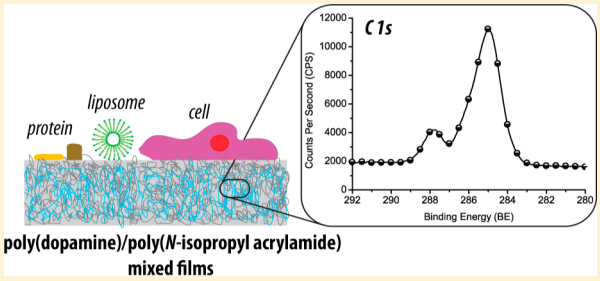

INTRODUCTION

Polymer coatings are of paramount importance for many biomedical applications from tissue engineering to implantable devices. There is a variety of different concepts used to equip surfaces interfacing with cells or tissue with a polymer film including polymer (self-assembled) monolayers,[1] thin films assembled via the sequential deposition of interacting polymers (the layer-by-layer (LbL) technique),[2] or poly(dopamine) (PDA) films.[3] The major biomedical purpose of these coatings aims to gain control over cell adhesion, proliferation, and differentiation. The approaches to achieve this are manifold and include the use of film charge and/or mechanics or the immobilization of specific antibodies or low-fouling polymers. Trapping active therapeutic compounds in these polymer coatings further optimizes their performance by administering drugs in a surface-mediated manner.[4] Entrapping drug deposits such as polymersomes into surface-adherent hydrogels[5] or liposomes,[6,7] cyclodextrins,[8] or micelles[9] into polymer thin films are advanced concepts to engineer better control over retention and release of therapeutic compounds.

PDA coatings have lately attracted considerable interest for a variety of biomedical applications from drug delivery or tissue engineering to biosensing.[3,10] The self-polymerization of dopamine at slight basic pH into PDA has first been reported in 2007 by Lee et al.[11] This approach has many advantages such as simple and fast deposition onto virtually any surface, the opportunity for postfunctionalization via thiols and amines, biocompatibility, no inherent cytotoxicity, and so forth. However, the details of the assembly mechanism and the PDA structure remain to be unambiguously identified. Speculations to this end include the entire spectra of possibilities from a covalent model[11] to a model which proposed the absence of any covalent linkages.[12] There are also recent models proposed which suggest the coexistence of both covalent and noncovalent interactions.[13,14] The assembly of PDA films has been characterized and compared varying different parameters. Apart from silica, hydrophobic substrates have attracted considerable interest due to the unique ability of PDA to be also formed on these substrates. Jiang et al. found that the organic substrates were more favorable for PDA deposition than silica, increasing the assembly temperature led to lower water contact angles, while it was difficult to identify a trend for the comparison of PDA films assembled on different organic substrates using different dopamine concentrations.[15] Good long-term stability of PDA films on hydrophobic substrates has also been reported.[16] PDA coatings have

Received: June 4, 2013
Revised: July 10, 2013
Published: July 15, 2013

commonly been postmodified with other molecules, for example, proteins via the inherent ability of the quinones in the film to react with thiols and/or amines via Michael addition and/or Schiff base addition.[11,17−19] Alternatively, the reactants can be premodified prior to the film assembly. Poly-(*L*-glutamic acid),[20] poly(aspartamide),[21] or the atom-transfer radical-polymerization initiator 2-bromoisobutyryl bromide[22] have been dopamine-modified and used for this purpose. The third option to expand/modify the properties of PDA coatings is by mixing the additional component into the dopamine solution prior to the film deposition. This approach has the advantage that no chemical modification or an additional adsorption step is required. However, there are only few reports where PDA was codeposited with another compound, for example, the copolymer poly(ethylene imine)−graft-poly-(ethylene glycol).[23] We recently demonstrated that poly-(ethylene glycol) and poly(vinyl alcohol) could be incorporated into PDA films by simple mixing, without the need of covalent linkages such as thiols or amines, giving further evidence that noncovalent forces could majorly contribute to the film assembly procedure.[24] In terms of applications, these results open up the possibility to assemble PDA based response films (e.g., pH or temperature responsive) possibly similar to coatings assembled via the LbL technique.[2] Interestingly, we also identified the first material, namely, poly(vinyl pyrrolidone) (PVP), which hinders PDA formation. We attributed this finding to the strong hydrogen acceptor property of PVP, which is probably stopping the PDA formation in a very early stage.

Poly(*N*-isopropylacrylamide) (pNiPAAm)[25] is a thermoresponsive polymer with a lower critical solution temperature (LCST) near physiological temperature in neutral pH, which makes it applicable in biomedicine. Among them, cell sheet engineering is a prominent example where a confluent cell layer cultured at 37 °C can be entirely detached upon decreasing the temperature.[26] This and other applications rely on the assumption that the interaction of proteins with pNiPAAm films changes at the LCST; that is, below the LCST proteins are repelled and above the LCST proteins adsorb. However, it turned out that the grafting density and the molecular weight of pNiPAAm affect the protein adsorption above the LCST.[27−30] Apart from pNiPAAm single component thin films, multilayered films using pNiPAAm as a building block have been considered to assemble (partly) thermoresponsive coatings.[31−34] The reader is referred to the comprehensive review by Tokarev and Minko for a more detailed overview over pNiPAAm coatings/materials.[35]

In this article, we studied the assembly of films consisting of PDA and aminated and carboxylated pNiPAAm (pNiPAAm-x, x = NH_2 or COOH) with the aim to assess if a thermoresponsive polymer can be mixed into a PDA coating and to characterize the properties of the mixed films (Scheme 1). Specifically, we (i) characterized the film assembly of PDA and pNiPAAm-x at 24 and 39 °C on gold and silica surfaces using a quartz crystal microbalance with dissipation monitoring (QCM-D), (ii) analyzed the composition of these films on silica surfaces using X-ray photoelectron spectroscopy (XPS), (iii) assessed the transparency of these coatings by UV−vis spectroscopy, (iv) visualized these coatings using atomic force microscopy (AFM), and (v) determined the adsorption of liposomes and proteins as well as the myoblast cell adhesion to the different coatings.

Scheme 1. Schematic Illustration of the Film Assembly Using Aminated or Carboxylated pNiPAAm (pNiPAAm-x) and DA[a]

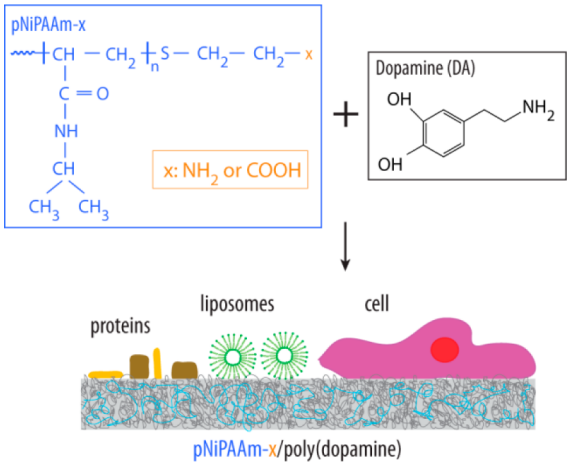

[a]The films are deposited on planar substrates and the adsorption of proteins, liposomes, or myoblast cells depending on the adsorption protocol and film composition are monitored.

EXPERIMENTAL SECTION

Materials. Aminated poly(*N*-isopropylacrylamide) (pNiPAAm-NH_2, MW = 2500 Da), carboxylated poly(*N*-isopropylacrylamide) (pNiPAAm-COOH, MW = 2000 Da), dopamine hydrochloride (DA), hydrofluoric acid (HF), tris(hydroxymethyl)aminomethane (TRIS), sodium chloride (NaCl), ethanol, and chloroform (pty ≥99.5%) were purchased from Sigma-Aldrich. Zwitterionic lipids 1-palmitoyl-2-oleoyl-*sn*-glycero-3-phosphocholine (POPC), negatively charged lipids 1-palmitoyl-2-oleyl-*sn*-glycero-3-phospho-L-serine (sodium salt) (POPS), positively charged lipids 1-palmitoyl-2-oleoyl-*sn*-glycero-3-ethylphosphocholine (POEPC), and fluorescent lipids 1-oleoyl-2-[6-[(7-nitro-2−1,3-benzoxadiazol-4-yl)amino]hexanoyl]-*sn*-glycero-3-phosphocholine (NBD-PC) were purchased from Avanti Polar Lipids (Alabaster, AL, USA).

TRIS buffer consisting of 10 mM TRIS (pH 8.5) was used throughout all of the experiments. The buffer solution was made with ultrapure water (Milli-Q gradient A 10 system, resistance 18 MΩ cm, TOC < 4 ppb, Millipore Corporation, Billerica, MA, USA).

Unilamellar liposome stock solutions were prepared by evaporation of the chloroform of 2.5 mg of lipid solution under vacuum for 1 h, followed by hydration into 1 mL of TRIS buffer and extrusion through 100 nm filters (11 times). Zwitterionic liposomes (L^{zw}) consisted of 2.5 mg of POPC lipids; negatively charged liposomes (L^-) were made from 0.5 mg of POPS and 2 mg of POPC lipids, and positively charged liposomes (L^+) consisted of 0.5 mg of POEPC and 2 mg of POPC lipids. For fluorescent liposomes, 1 wt % NBD-PC was added to the lipid solution.

LCST Determination. The LCST of pNiPAAm-NH_2 (0.7 mg mL^{-1} in TRIS buffer) and pNiPAAm-COOH (0.5 mg mL^{-1} in TRIS buffer) solutions was determined by measuring the absorbance of the solution at 547 nm using a temperature-controlled multiplate reader (Perkin Elmer).

Sample Preparation and Analysis. Samples of 1 × 1 cm^2 pieces of silica wafer (XPS, AFM, CA), 1.8 × 1.8 cm^2 glass slides (UV−vis), or 2.5 cm diameter glass slides (CLSM) were cleaned by sonication in ethanol for 10 min followed by 10 min in MQ water. The samples were then blow-dried under a stream of nitrogen and put in a UV/ozone cleaner for 15 min. The cleaned samples were then instantly coated with DA (1 mg mL^{-1} in TRIS buffer), pNiPAAm-x (0.7 mg mL^{-1} for pNiPAAm-NH_2, 0.5 mg mL^{-1} for pNiPAAm-COOH in TRIS buffer), or a DA/pNiPAAm-x mixture (molar ratio 1/1, 5/1, and 20/1, 25/1 DA/pNIPAAm-NH_2, at a DA concentration of 1 mg mL^{-1} in TRIS buffer) for 1 h with exchanging the solution after 30 min.

dx.doi.org/10.1021/la402118u | *Langmuir* 2013, 29, 10213−10222

Alternatively, the cleaned silica substrates were coated with DA (1 mg mL^{-1} in TRIS buffer) for 1 h with exchanging the solution after 30 min followed by the adsorption of pNiPAAm-x (0.7 mg mL^{-1} for pNiPAAm-NH_2, 0.5 mg mL^{-1} for pNiPAAm-COOH in TRIS buffer) for 30 min. Samples with a coating temperature of 39 °C were prepared by putting the solution and silica substrate in a plastic tube and on a thermoshaker (Thermomixer comfort, Eppendorf). The coated samples were rinsed with MQ water, dried under a stream of nitrogen, and stored under vacuum for further analysis.

X-ray Photoelectron Spectroscopy (XPS). XPS data acquisition was performed using a Kratos Axis UltraDLD instrument (Kratos Analytical Ltd., Telford, UK) equipped with a monochromated Alkα X-ray source ($h\nu$ = 1486.6 eV) operating at 15 kV and 10 mA (150 W). Survey spectra (binding energy (BE) range of 0−1400 eV with a pass energy of 160 eV) were used for element identification and quantification. High-resolution C 1s, O 1s, and N 1s spectra were acquired with a pass energy of 20 eV. The acquired data were converted to VAMAS format and analyzed using CasaXPS (Casa software Ltd., UK) software. Three areas of at least two independent samples were analyzed to test the homogeneity of the films.

Ellipsometry (ELM). The thickness of the films was assessed by ELM (ELX-02C) using wavelength λ = 632.8 nm and an angle of incidence of 70°. The thickness was modeled using a three layer model assuming a refractive index of the organic layer n = 1.55.

Atomic Force Microscopy (AFM). The coatings on the silica wafers were visualized in air using tapping mode AFM (Nanowizard 2, JPK Germany) using NCH cantilever (NanoWorld). The roughness (root-mean-squared (RMS)) was analyzed from at least two independent 5 × 5 μm^2 images using the JPK software.

Absorbance Measurements. The glass slides were mounted in a UV/vis spectrometer (UV-3600, Shimadzu), and the absorbance was monitored from 350 to 1200 nm.

Contact Angle Measurements (CA). The water CA of the different coatings was measured at 24 °C (DSA100, Krüss) using the "tangent method 2" in the Drop Shape Analysis software.

Confocal Laser Scanning Microscopy (CLSM). Fluorescent recovery after photobleaching (FRAP) experiments were conducted using a Zeiss Axiovert microscope coupled to an LSM 700 confocal scanning module (Carl Zeiss, Germany). The coated glass slides were mounted in a liquid cell and covered with TRIS buffer solution followed by the exposure to a solution of L^{zw} for 30 min and three washing steps. The fluorescence was bleached in a small area, and the recovery of the bleached area was observed.

Quartz Crystal Microbalance with Dissipation Monitoring (QCM-D). QCM-D measurements (Q-Sense E4, Sweden) were used to analyze the assembly of the polymer coatings and the subsequent adsorption proteins and liposomes. Gold and silica-coated crystals (QSX300, Q-Sense) were cleaned by immersion in a 2 wt % sodium dodecyl sulfate solution overnight and rinsing with Milli-Q water. Afterward, the crystals were blow-dried with N_2, treated with UV/ozone for 20 min, and mounted into the liquid exchange chambers of the instrument. The frequency and dissipation measurements were monitored at 24 ± 0.02 °C or 39 ± 0.02 °C. When a stable baseline in TRIS buffer solution was achieved, either DA (1 mg mL^{-1}), pNiPAAm polymer (0.7 mg mL^{-1} for pNiPAAm-NH_2 and 0.5 mg mL^{-1} for pNiPAAm-COOH), or DA/pNiPAAm polymer mixture (1 mg mL^{-1} DA, pNiPAAm-NH_2 0.7 mg mL^{-1}, and pNiPAAm-COOH 0.5 mg mL^{-1}) were introduced into the measurement chamber and left to adsorb onto the crystal until the surface was saturated. Then, the chamber was rinsed with TRIS buffer and the selected coatings where exposed to either a protein solution (Dulbecco's modified Eagle's medium plus 10% fetal bovine serum) or a liposome solution (stock solution). Alternatively, the crystals were precoated with either DA (1 mg mL^{-1}) for 10 or 60 min, DA/pNiPAAm-NH_2 polymer mixture (1 mg mL^{-1} DA and 0.7 mg mL^{-1} pNiPAAm-NH_2) at 24 or 39 °C, or first with DA (1 mg mL^{-1}) for 60 min followed by pNiPAAm-NH_2 (0.7 mg mL^{-1}) for 30 min prior to the mounting in the QCM chamber. Normalized frequencies using the third harmonic are presented. The differences of protein absorption and liposome absorption were statistically analyzed using an unpaired two-tailed *t*-test.

Cell Experiments. The C2C12 mouse myoblast cell line (American Type Culture Collection) was used for the experiments. The cells (150 000 cells/flask in 20 mL medium) were cultured in 75 cm^2 culture flasks in medium (Dulbecco's modified Eagle's medium with Glutamax (DMEM) supplemented with 10% fetal bovine serum, 50 μg mL^{-1} penicillin, 50 μg mL^{-1} streptomycin, and 1 mM sodium pyruvate, all from Invitrogen) at 37 °C and 5% CO_2.

Cell Adhesion. 9 mm diameter glass slides were cleaned and dried as previously described. (For details on the sample coating see Supporting Information.) The coated glass slides were sterilized in 70% ethanol for 5 min followed by 3× washes in sterile PBS buffer. The cells were seeded at a density of 50 000 cells/well in 2 mL of medium and allowed to attach for 24 h at 37 °C and 5% CO_2. After the incubation time, the cells were washed 3× with 3 mL of PBS and fixed using 4% paraformaldehyde solution for 20 min followed by multiple PBS washing steps. (For details on the cell staining see Supporting Information.) Fluorescent images of fixed cells were taken using an Olympus CKX41 microscope equipped with the corresponding filter sets and a 10× objective. At least six pictures per substrate were taken to assess the number of adhering cells per surface area depending on the underlying substrate.

RESULTS AND DISCUSSION

LCST Determination. Prior to the film assembly, the LCST of pNiPAAm-x was assessed via turbidity measurements (Supporting Information, Figure S1). Both polymers had a LCST above 40 °C, probably due to the presence of the charged end groups on the low molecular weight polymers which might be contributing to the solubility of the polymers. Further, the transition for pNiPAAm-NH_2 was sharper than for pNiPAAm-COOH. However, since we are aiming to use these coatings for biomedical applications, two temperatures, 24 and 39 °C, below the LCST were chosen for their assembly. The latter case was purposefully selected at the border where the polymers started to precipitate, expecting different film assembly behavior at this temperature compared to 24 °C.

Film Assembly. With the aim to understand to what extent the presence of pNiPAAm-x is affecting the PDA film deposition, gold and silica QCM crystals with or without PDA precoating were exposed to different polymer solutions, that is, DA, DA/pNiPAAm-x, or pNiPAAm-x at 24 or 39 °C (DA/24(39), DA/pNiPAAm-x/24(39), or pNiPAAm-x/24(39)). Figure 1 gives an overview over the changes in frequency (Δf) of the crystals exposed to these solutions. (For the corresponding changes in dissipation ΔD, see Supporting Information, Figure S2). From literature, one would expect that the aminated polymer is preferentially incorporated into the films since it has the ability to form covalent linkages with the quinones of the PDA.[11] There was more PDA deposited onto Au surfaces than onto silica at 24 °C, but there was no difference between the two adsorption temperatures observed. While pNiPAAm-x adsorbed onto gold but not onto silica at 24 °C, a deposition temperature of 39 °C yielded a Δf of over 1000 Hz and around 70 Hz of the silica crystal for pNiPAAm-NH_2 and for pNiPAAm-COOH, respectively. This could be explained due to the fact that, at 39 °C, the configuration of pNiPAAm-x is changing toward its hydrophobic (collapsed) state and (partly) precipitates onto the surface, while at 24 °C pNiPAAm-x is in its water-soluble hydrophilic state. Δf for pNiPAAm-NH_2/39 was larger as compared to pNiPAAm-COOH/39, probably because the MW of the carboxylated polymer is slightly lower than for the aminated one. MW is known to affect the LCST of polymers,[36,37] which can also be

dx.doi.org/10.1021/la402118u | Langmuir 2013, 29, 10213−10222

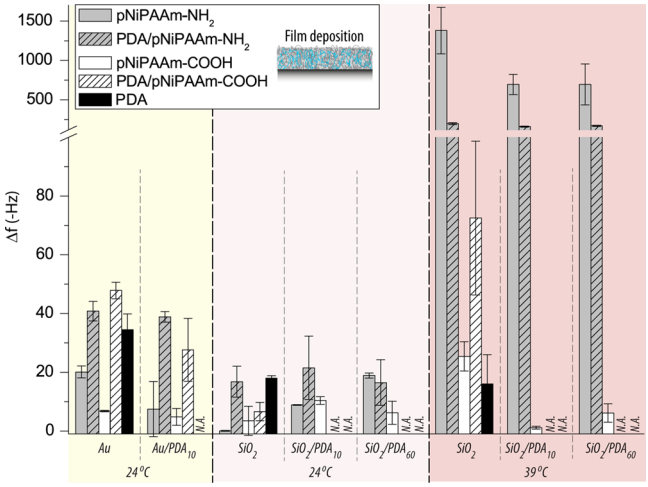

Figure 1. Frequency changes (Δf) of bare Au or SiO_2 or PDA precoated QCM-D crystals upon coating with different polymers and polymer mixtures at 24 and 39 °C is shown. (The molar ratio of DA/pNiPAAm-x is 20/1 for all measurements.)

seen from our LCST determination of pNiPAAm-NH_2 and pNiPAAm-COOH (Supporting Information, Figure S1). Alternatively, the end groups could affect the conformation change of the polymer, an effect previously observed for pNiPAAm. It has been speculated that MW and end groups affect the hydration of the polymer due to different interactions with water molecules.[38,39] Precoating gold or silica crystals with PDA allowed for the adsorption of pNiPAAm-x/24 in both cases. Interestingly, for PDA precoated silica crystals, the pNiPAAm-x/39 adsorption was reduced as compared to bare silica. This could be due to the fact that the sites for interactions were less accessible when the polymer is in its collapsed form. Further, although Δf for pNiPAAm-NH_2/39 onto PDA precoated crystals was reduced by 50% as compared to bare silica, it was still ∼ −750 Hz, while for pNiPAAm-COOH/39 Δf was close to zero, again demonstrating the effect of either the difference in either MW or end groups.

When considering the deposition of the mixtures, there was a larger Δf for PDA/pNiPAAm-NH_2/24 than for PDA/pNiPAAm-COOH/24 measured when deposited onto silica crystals, while there was only a small difference when gold crystal were used. In the latter case, Δf for DA/pNiPAAm-x/24 was similar to PDA/24, making it impossible to conclude if only PDA or PDA/pNiPAAm-x was formed on the surface. A similar conclusion can be drawn when comparing PDA/24 to PDA/pNiPAAm-NH_2/24 deposition onto silica. On the other hand, the deposition of PDA/pNiPAAm-NH_2/39 onto silica was higher than at 24 °C and exhibited higher adsorption kinetics (Supporting Information, Figure S3). The measured Δf for PDA/pNiPAAm-NH_2/39 was larger and smaller than for PDA/39 and pNiPAAm-NH_2/39, respectively. The former observation indicates that a mixed film was deposited. Further, the lower Δf for PDA/pNiPAAm-NH_2/39 than for pNiPAAm-NH_2/39 could be due to the fact that the presence of the DA molecules was affecting the phase transition of the polymer or the presence of the pNiPAAm-NH_2 on the surface was slowing down the PDA growth. The deposition of PDA/pNiPAAm-COOH/39 was higher than PDA/39 and pNiPAAm-COOH/39. This suggests that a mixed coating was assembled and that the pNiPAAm-COOH/39 and DA/39 were not affecting each other in their ability to assemble a film.

When considering PDA precoated crystals, the adsorption of pNiPAAm-COOH/39 was already low, and therefore, only PDA/pNiPAAm-NH_2/39 mixtures were considered. Δf for PDA/pNiPAAm-NH_2 observed was independent of the tested PDA precoating time, but only dependent on the deposition temperature. The higher temperature led to larger changes in Δf as expected.

With the aim to get more detailed insight into the elemental composition of the deposited films, XPS analysis was performed on coated silica substrates. Silica substrates were considered because according to the QCM results, they did not allow for the adsorption of pNiPAAm-x only, facilitating the XPS spectra analysis. Figure 2a shows the C 1s high resolution scans for bare silica and silica exposed to pNiPAAm-x/24, confirming the QCM results that no pNiPAAm-x adsorbed to silica at 24 °C.

By comparing the C 1s spectra of PDA/24 and PDA/pNiPAAm-x/24 mixtures (Figure 2b), the expected increase in the carbonyl peak (C=O) at 287.8 eV for PDA/pNiPAAm-x/24 and the low level of pNiPAAm-x/24 adsorbed onto silica suggest that the deposition of a PDA/pNiPAAm-x/24 mixed film was likely. This was further supported by the increase in intensity for the aliphatic carbon (C-C, C-H) at 285 eV when comparing PDA/24 to PDA/pNiPAAm-x/24. It further suggests that the different end-groups on the pNiPAAm were affecting the film deposition; that is, pNiPAAm-NH_2 seemed to promote the film adsorption to greater extent than pNiPAAm-COOH, probably due to the ability of the amines to couple to the quinones of the PDA. It is quite surprising that pNiPAAm-COOH was detected in the coatings at all, since this polymer does not have any amines or thiols, but seems to be trapped via noncovalent interactions only. When comparing PDA/pNiPAAm-NH_2/39 films to PDA/pNiPAAm-NH_2/24, the higher intensity of the aliphatic carbon and the carbonyl peak implies larger mass deposition in the former case in good agreement with the QCM results.

By comparing the C 1s spectra of PDA/24 to the subsequent deposition of PDA/24 (coating time 60 min) and pNiPAAm-x/24 (PDA_{60}-pNiPAAm-x/24, Figure 2c), there was only a small difference in peak intensities at BE ∼287.8 and 285 eV when comparing PDA/24 to PDA_{60}-pNiPAAm-x/24, independent of the end group of the pNiPAAm-x.

The results from the C 1s high resolution scans are further supported by the change in elemental composition by comparing PDA/24 to PDA/pNiPAAm-x/24(39) and PDA_{60}-pNiPAAm-x/24 (Table 1). The expected decrease in O/C ratio and increase in N/C and N/O ratios was observed for PDA/24 vs PDA/pNiPAAm-x/24 and PDA_{60}-pNiPAAm-x/24 films. When employing DA/pNiPAAm-x mixtures, the decrease in O/C ratio was more pronounced for the aminated pNiPAAm as compared to the carboxylated polymer, indicating larger film deposition in the former case. The change in these ratios was more evident when the mixed film was deposited at 39 °C as compared to 24 °C, supporting our QCM results that elevated temperatures were promoting the film formation. Further, films assembled via the subsequent adsorption of PDA and pNiPAAm-x at 24 °C showed a similar decrease and increase in O/C and N/C or N/O independent of the end group of the pNiPAAm. This finding is in agreement with the QCM results and suggests that the quinone/amine interaction is not the major way of pNiPAAm-x immobilization onto PDA. Additionally, the elemental % of Si 2p was found to be lower for PDA/pNiPAAm-x/24 and PDA_{60}-pNiPAAm-x/24 than pNi-

dx.doi.org/10.1021/la402118u | Langmuir 2013, 29, 10213−10222

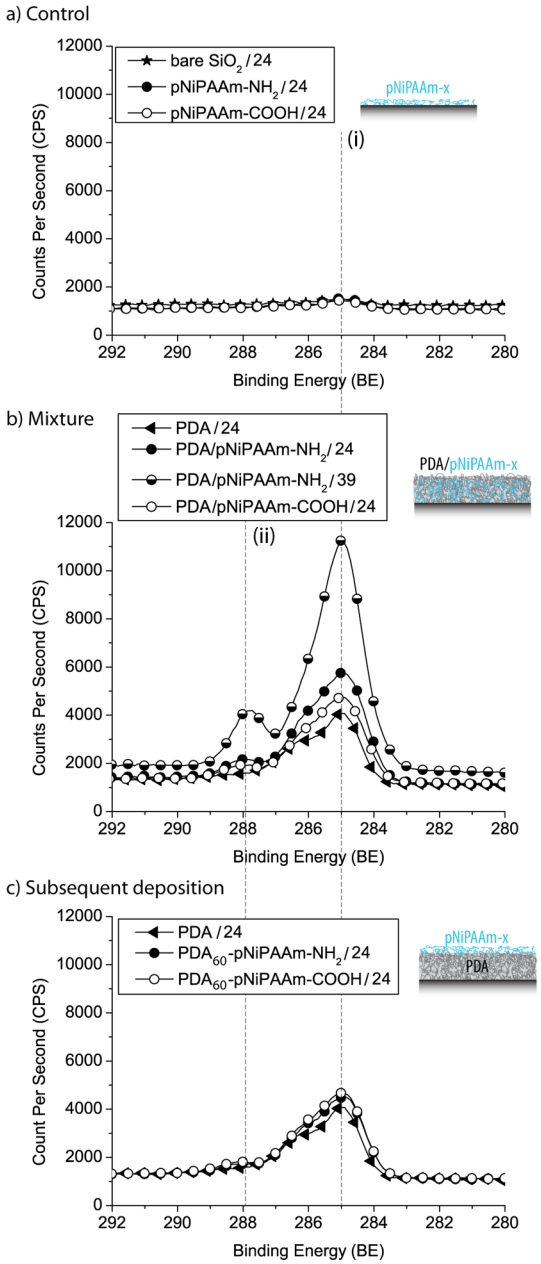

Figure 2. C 1s peak of different coatings as monitored by XPS: (a) deposition of pNiPAAm-x/24 onto SiO_2, (b) deposition of PDA/pNiPAAm-x/24(39) onto SiO_2, and (c) deposition of PDA_{60} followed by pNiPAAm-x/24 onto SiO_2. The highlighted regions in C 1s are (i) the C-C/C-H region at BE = 285.0 eV and (ii) the C=O region at BE ≈ 287.8 eV. (The molar ratio of DA/pNiPAAm-NH_2 is 20:1 for all measurements.)

PAAm-x/24 only, indicating that the mixtures have been deposited on the surface.

With the aim to substantiate the XPS results, the transparency of the coatings was assessed by UV−vis spectroscopy (Figure 3). The absorbance of PDA/24(39) coating was compared to PDA/pNiPAAm-x/24(39) films. The absorbance was found to be similar for PDA/24 and PDA/pNiPAAm-x/24. Although the crystal in the QCM experiments exhibited similar Δf for PDA/24 and PDA/39, the PDA/39 was found to be optically denser as compared to PDA/24. Further, when comparing the coatings assembled at 39 °C, the absorbance for PDA/39 was higher than for the mixtures, implying that the optical density was reduced by the presence of the pNiPAAm-x in the film. These findings are in agreement with the XPS results and suggest the deposition of mixed PDA/pNiPAAm-x films for both end groups.

ELM was employed to assess the dry thickness of the different coatings using different deposition temperatures and a coating time of 60 min (Supporting Information, Table S1). The overall thin coatings can be explained by the short deposition time. When comparing the deposition at 24 °C, PDA had a slightly higher thickness than the mixed films. The similarly thickest coatings were obtained when first PDA_{60} was deposited followed by the adsorption of pNiPAAm-x at 24 °C. When comparing PDA/pNiPAAm-NH_2 deposited at 24 and 39 °C, only a slight increase in dry thickness was observed in the latter case. The difference between the ELM and the QCM-D experiments could be explained by the fact that, in the former case, dry films were analyzed, while in the latter case, the water contents were considered. This implies that the mixed films deposited at 39 °C were highly hydrated.

We visualized the topography of the different coatings using AFM. PDA/24(39) and pNiPAAm-x/24(39) films were compared to PDA/pNiPAAm-x/24(39) films (Figure 4). To quantitatively compare the different films, the roughness was analyzed. The mixed films exhibited a lower roughness, with some larger aggregated in a smooth background, compared to a bare PDA film when deposited at 24 °C. Since we previously showed that pNiPAAm-NH_2/24 only adsorbed in very low amounts onto silica, the low roughness was expected. On the other hand, when the films were deposited at 39 °C, the roughness for PDA/39 and PDA/pNiPAAm-NH_2/39 coatings was found to be lower than for these films deposited at 24 °C. Further, the roughness decreased from PDA/39 to PDA/pNiPAAm-NH_2/39 to pNiPAAm-NH_2/39 coatings. The roughness of pNiPAAm-NH_2/39 films was very low, and together with the QCM-D results, we concluded that was due to the high amount of adsorbed polymer. Surprisingly, PDA/pNiPAAm-COOH/39 coatings had the highest roughness from all of the films deposited at 39 °C.

Due to observed decrease in roughness when comparing PDA/39, PDA/pNiPAAm-NH_2/39, and pNiPAAm-NH_2/39 coatings, we assembled films with different DA/pNiPAAm-NH_2/39 ratios and visualized them by AFM with the aim to image the transition from a PDA/39 to a pNiPAAm-NH_2/39 coating (Figure 5). With an increasing amount of pNiPAAm-NH_2, the mixed films had a lower and lower roughness. This demonstrates that we can gradually change the property of the film by adjusting the mixing ratio between the two components.

The water CA of PDA/24(39), pNiPAAm-NH_2/24(39), PDA/pNiPAAm-NH_2/24(39), and PDA_{60}-pNiPAAm-NH_2/24(39) films was measured at 24 °C to assess their wettability (Supporting Information, Table S2). Interestingly, the CA angle for PDA/24 was slightly higher than for PDA/39 hinting toward a difference in the coating properties depending on the deposition temperature. pNiPAAm-NH_2/24(39) were equally hydrophilic. In the former case, a very low amount of the polymer was adsorbed as seen from the XPS and QCM-D experiments, which suggests that the CA of silica was measured. In the latter case, the polymer was in its hydrophilic state, which together with the low roughness value determined by AFM led likely to the low measured CA. The CA for PDA/pNiPAAm-NH_2/24 was lower than for PDA/pNiPAAm-NH_2/39. In the latter case, the higher amount of deposited pNiPAAm-NH_2 might affect the wettability of the film. A

dx.doi.org/10.1021/la402118u | Langmuir 2013, 29, 10213−10222

Table 1. Atomic Composition of Different Coatings Assembled on Silica Wafer as Determined by XPS[a]

	elemental %	C	O	N	Si
plain films	SiO_2	4.09 ± 0.78	42.68 ± 1.06	0.00 ± 0.00	53.24 ± 1.82
	pNiPAAm-NH_2	7.83 ± 2.58	40.68 ± 1.85	0.00 ± 0.00	51.50 ± 0.90
	pNiPAAm-COOH	8.29 ± 2.61	40.87 ± 2.12	0.00 ± 0.00	50.84 ± 0.70
	PDA	35.87 ± 10.60	30.34 ± 3.38	3.99 ± 1.62	29.80 ± 8.84
mixed films	PDA/pNiPAAm-NH_2 24 °C	52.90 ± 9.38	24.65 ± 4.69	6.73 ± 1.35	15.71 ± 6.05
	PDA/pNiPAAm-NH_2 39 °C	56.82 ± 13.74	19.90 ± 6.21	8.66 ± 2.38	14.62 ± 9.89
	PDA/pNiPAAm-COOH	39.81 ± 10.13	27.89 ± 3.43	4.48 ± 2.00	27.83 ± 8.72
SD	PDA_{60}-pNiPAAm-NH_2	55.54 ± 3.84	23.53 ± 1.38	6.47 ± 0.69	14.47 ± 2.95
	PDA_{60}-pNiPAAm-COOH	55.59 ± 3.86	24.45 ± 0.88	6.46 ± 0.63	13.50 ± 3.89
	elemental %	O/C	N/C	N/O	N/Si	C/Si
plain films	SiO_2	10.72 ± 1.77	0.00 ± 0.00	0.00 ± 0.00	0.00 ± 0.00	0.08 ± 0.02
	pNiPAAm-NH_2	5.78 ± 2.15	0.00 ± 0.00	0.00 ± 0.00	0.00 ± 0.00	0.15 ± 0.05
	pNiPAAm-COOH	5.48 + 2.10	0.00 ± 0.00	0.00 ± 0.00	0.00 ± 0.00	0.16 ± 0.05
	PDA	0.94 ± 0.37	0.11 ± 0.01	0.14 ± 0.07	0.16 ± 0.10	1.40 ± 0.80
mixed films	PDA/pNiPAAm-NH_2 24 °C	0.49 ± 0.18	0.13 ± 0.00	0.29 ± 0.11	0.52 ± 0.29	4.06 ± 2.17
	PDA/pNiPAAm-NH_2 39 °C	0.21 ± 0.02	0.16 ± 0.01	0.76 ± 0.09	2.01 ± 0.77	12.84 ± 4.53
	PDA/pNiPAAm-COOH	0.76 ± 0.28	0.11 ± 0.02	0.17 ± 0.09	0.20 ± 0.14	1.67 ± 0.90
SD	PDA_{60}-pNiPAAm-NH_2	0.43 ± 0.05	0.12 ± 0.01	0.28 ± 0.04	0.47 ± 0.13	4.02 ± 1.08
	PDA_{60}-pNiPAAm-COOH	0.44 ± 0.04	0.12 ± 0.01	0.26 ± 0.03	0.52 ± 0.17	4.49 ± 1.55

[a]If not mentioned differently, the deposition temperature was 24 °C. (The molar ratio of DA/pNiPAAm-x is 20/1 for all measurements.) (SD: subsequent deposition).

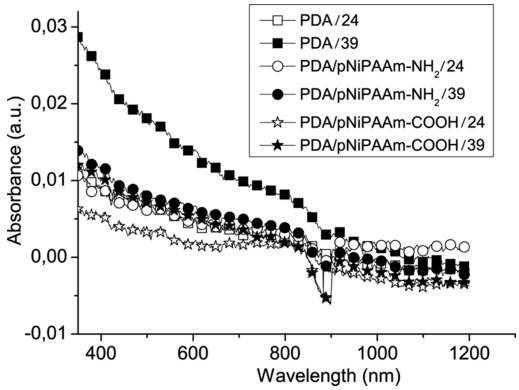

Figure 3. Representative UV−vis spectra of glass slides coated with PDA/24(39), PDA/pNiPAAm-NH_2/24(39), or PDA/pNiPAAm-NH_2/24(39). (The molar ratio of DA/pNiPAAm-x is 20/1 for all measurements.)

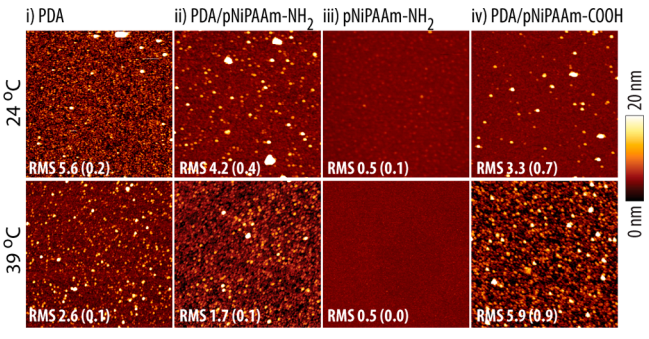

Figure 4. Representative tapping mode AFM images (5 × 5 μm^2) of PDA, PDA/pNiPAAm-NH_2, pNiPAAm-NH_2, or PDA/pNiPAAm-COOH deposited at 24 °C (top) or 39 °C (bottom). The roughness values [RMS (nm) and (standard deviation)] are mentioned on the bottom of the images. (The molar ratio of DA/pNiPAAm-x is 20:1 for all measurements.)

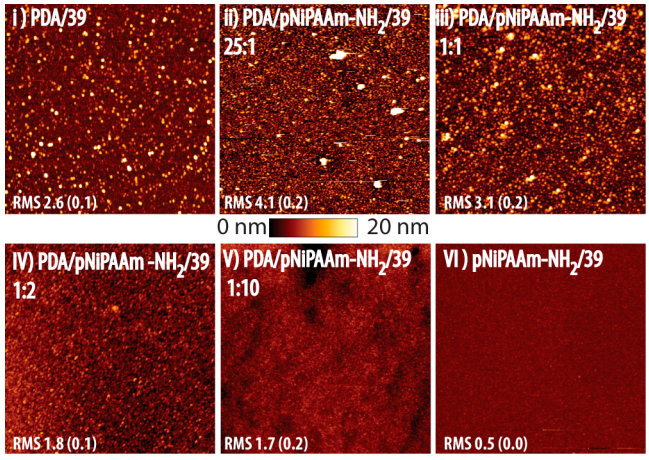

Figure 5. Representative tapping mode AFM images (5 × 5 μm^2) of PDA/pNiPAAm-NH_2/39 using different molar ratios of DA/pNiPAAm-NH_2. The roughness values [RMS (nm) and (standard deviation)] are mentioned on the bottom of the images.

similar trend could be observed for PDA_{60}-pNiPAAm-NH_2/24(39) films, indicating the presence of more pNiPAAm-NH_2 when deposited at 39 °C. Furthermore, PDA/24(39) showed a lower CA compared to the mixed films, likely due to the higher roughness in the latter case. The effect of roughness on contact angle measurements has first been considered by Wenzel in 1949,[40] and from there, many reports demonstrated that the CA of hydrophilic surfaces increases with increasing roughness, for example, by Herminghaus.[41]

Protein Adsorption. This section aims to assess if the coatings differ in their ability to interact with a protein mixture. Understanding the basic properties of biointerphases in this regard is an important aspect toward their biomedical consideration. Only pNiPAAm-NH_2 was used for the following experiments since it showed larger incorporation into the films.

Figure 6a shows Δf of PDA/24(39), PDA/pNiPAAm-NH_2/24(39), PDA_{60}-pNiPAAm-NH_2/24(39), or pNiPAAm-NH_2/

dx.doi.org/10.1021/la402118u | Langmuir 2013, 29, 10213−10222

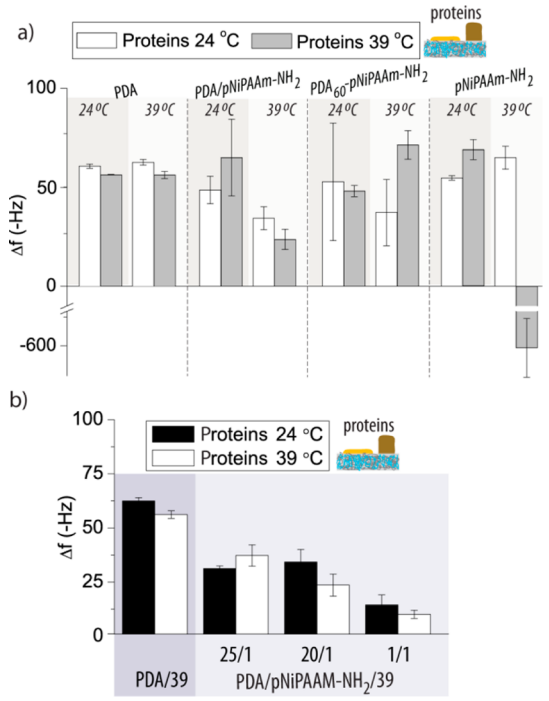

Figure 6. (a) Frequency changes (Δf) of a QCM crystal precoated with PDA/24(39), PDA/pNiPAAm-NH_2/24(39), PDA_{60}-pNiPAAm-NH_2/24(39), or pNiPAAm-NH_2/24(39) upon exposure to a protein solution at 24 or 39 °C. (The molar ratio of DA/pNiPAAm-NH_2 is 20:1 for all measurements.) (b) Frequency changes Δf of a QCM crystal precoated with PDA/pNiPAAm-NH_2/39 using different molar ratios of DA/pNiPAAm-NH_2 upon the exposure to a protein solution at 24 or 39 °C. Protein adsorption to PDA/39 is plotted for comparison.

24(39) precoated crystals upon protein adsorption at 24 and 39 °C. Proteins adsorbed in a similar amount to PDA films independent of the coating or protein adsorption temperature, showing that the pristine PDA coatings were not affected by the temperature. Mixed films PDA/pNiPAAm-NH_2/24 also allowed similar amounts of adsorbed proteins, independent of the protein adsorption temperature. On the other hand, PDA/pNiPAAm-NH_2/39 showed significantly lower protein binding as the previously mentioned films for both protein adsorption temperatures, suggesting that the pNiPAAm-NH_2 in the mixed film was affecting its properties. When considering films assembled by depositing PDA_{60} first followed by pNiPAAm-NH_2, there was no significant difference in protein adsorption between the tested temperatures. Interestingly, when considering the dissipation changes ΔD of the protein layers, they were as expected but for PDA_{60}-pNiPAAm-NH_2 (Supporting Information, Figure S4). The protein adsorption to this film exhibited a large ΔD, which is indicative for a soft, hydrated layer, since ΔD is a measure for the viscoelasticity of the film.[42] Further, we have previously shown that pNiPAAm-NH_2/24 did not adsorb to silica (Figures 1 and 2); therefore, it is not surprising that no effect of the protein adsorption temperature was found in this case. However, pNiPAAm-NH_2/39 was deposited in large amounts onto silica as demonstrated by our QCM results (Figure 1). Similar amounts of proteins as to PDA coated silica were found to adsorb to this coating at 24 °C, indicating that, despite the large amount of pNiPAAm-NH_2, no protein resistance was observed. On the other hand, when these coatings were exposed to a protein solution at 39 °C, a large positive Δf (and negative ΔD) was observed. This is indicative for mass loss from the surface,[43−45] probably due to the displacement of the pNiPAAm-NH_2 by the proteins.

Next, we aimed to understand if the different molar ratios between DA and pNiPAAm-NH_2 affect the amount of adsorbed proteins. QCM crystals coated with PDA/pNiPAAm-NH_2/39 using different molar ratios of DA to pNiPAAm-NH_2 were exposed to a protein solution at 24 and 39 °C. Only PDA/pNiPAAm-NH_2/39 films were used since they exhibited larger pNiPAAm-NH_2 incorporation than PDA/pNiPAAm-NH_2/24. Figure 6b shows Δf of the precoated crystals upon exposure to proteins. The results for PDA/39 are plotted as comparison. With increasing amount of pNiPAAm-NH_2 in the films, the protein adsorption decreased for both protein adsorption temperatures. This was expected for protein adsorption at 24 °C due to the hydrated state of pNiPAAm-NH_2. It is surprising for 39 °C as the protein adsorption temperature, since the state of the pNiPAAm-NH_2 was expected to change when approaching the LCST. It might indicate that the ability of the pNiPAAm-NH_2 chains to collapse was affected when codeposited with PDA. Importantly, these results showed that it is possible to not only implement pNiPAAm-NH_2 into the films, but that there is also control over the properties depending on the mixing ratio.

Liposome Adsorption. Liposomes are important for various biomedical applications ranging from biosensing[46] to drug delivery.[47,48] Due to their lipid bilayer structure, liposomes are considered as simple mimics of biological cells and are therefore important in the context of biointerphases and their modification. In here, we assess the liposome adsorption to the different PDA and pNiPAAm-NH_2 coatings.

Figure 7a shows Δf of PDA/24(39), PDA/pNiPAAm-NH_2/24(39), PDA_{60}-pNiPAAm-NH_2/24(39), or pNiPAAm-NH_2/24(39) precoated crystals upon zwitterionic liposome (L^{zw}) adsorption at 24 and 39 °C. The L^{zw} deposition at both temperatures to all coatings was found to be similarly low with the exception of PDA/39. In the latter case, high L^{zw} adsorption was observed indicating that the properties of the PDA coating were affected by the deposition temperature when considering L^{zw} adsorption. Since the amount of deposited L^{zw} at 24 and 39 °C to PDA/39 was similarly large, it is unlikely that the different temperatures were affecting the properties of the liposomes in their ability to adsorb to PDA. With exception of PDA/39, it is therefore difficult to conclude from the QCM data if intact L^{zw} were deposited due to the low Δf and ΔD (Supporting Information Figure S5). Low Δf and ΔD for L^{zw} adsorption were also monitored for the films assembled using different ratios between DA and pNiPAAm-NH_2 (Supporting Information, Figure S6). To further address this aspect, CLSM images were taken of all of the coatings after fluorescently labeled L^{zw} were adsorbed at 24 °C (Figure 7b). In good agreement with the QCM results, similarly fluorescent intensities were monitored for all the coatings with the exception of PDA/39 which exhibited a much higher intensity. Samples coated with pNiPAAm-NH_2 appeared in general brighter likely due to the absence of PDA which is known to interfere with fluorescence readings. In addition, FRAP experiments were conducted by photobleaching a small area. No recovery of the fluorescence was observed after 10 min, suggesting that a low amount of intact L^{zw} was present and not supported lipid bilayers.

With the aim to get a more detailed understanding of the fact that PDA/24 allowed only low L^{zw} adsorption while a much

dx.doi.org/10.1021/la402118u | Langmuir 2013, 29, 10213−10222

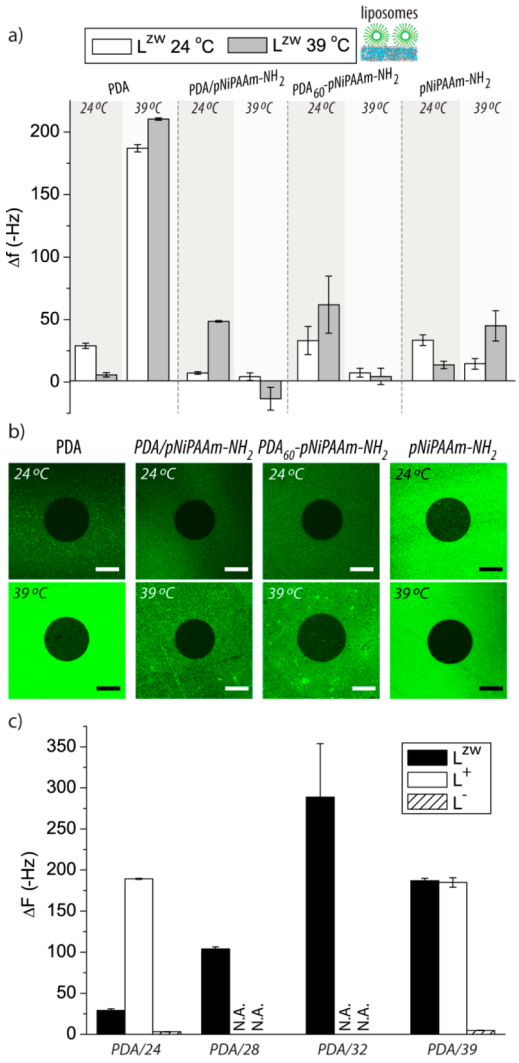

Figure 7. (a) Frequency changes (Δf) of a QCM crystal precoated with PDA/24(39), PDA/pNiPAAm-NH_2/24(39), PDA_{60}-pNiPAAm-NH_2/24(39), or pNiPAAm-NH_2/24(39) upon exposure to a L^{zw} solution at 24 or 39 °C. (b) Fluorescent confocal microscopy images of fluorescently labeled L^{zw} adsorbed onto the different coatings including a photobleached spot. All of the images were taken using the same settings, but PDA/39 which has a 60% lower gain, 5 min after photobleaching. The scale bar is 10 μm. (The molar ratio of DA/pNiPAAm-NH_2 is 20/1 for all measurements in a and b.) (c) Frequency changes (Δf) of a QCM crystal precoated with PDA deposited at different temperatures followed by the adsorption of L^{zw}, L^+, or L^-.

larger amount of L^{zw} was deposited onto PDA/39, we deposited PDA at two different intermediate temperatures, 28 and 32 °C, and adsorbed L^{zw} at 24 °C to these coatings. The fascinating results were that the amount of deposited L^{zw} was dependent on the PDA deposition temperature (Figure 7c). On the other hand, when using positively or negatively charged liposomes (L^+ and L^-, respectively), there was no PDA deposition temperature-dependent adsorption of the liposomes observed. L^+ and L^- were always immobilized in a high and low manner, respectively. This confirms the previously reported negative net charge of these PDA coatings.[49] It however cannot be the only reason for the different adsorption behavior of L^{zw}. In addition to that, it also showed that the PDA coating temperature was affecting the film properties. This interesting observation will further contribute to the wide application of PDA coatings.

Myoblast Cell Adhesion. With the aim to test these coatings *in vitro*, myoblast cells were allowed to adhere to PDA/24(39), PDA/pNiPAAm-NH_2/24(39), PDA_{60}-pNiPAAm-NH_2/24(39), and pNiPAAm-NH_2/24(39) coatings for 24 h, and they were counted and visualized (Figure 8). There

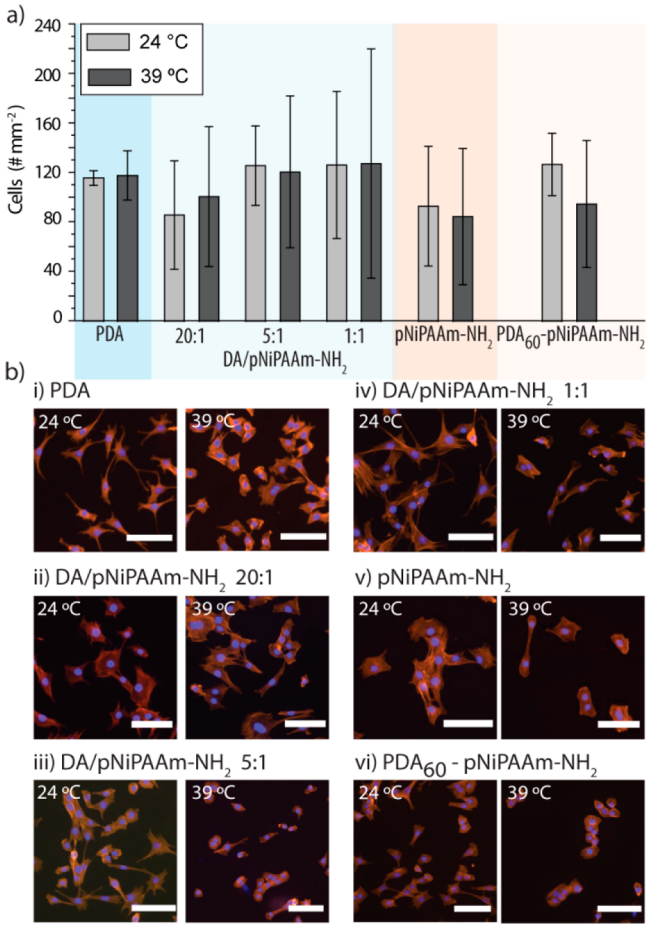

Figure 8. (a) Number of myoblast cells after 24 h adhering to PDA/24(39), PDA/pNiPAAm-NH_2/24(39), pNiPAAm-NH_2/24(39), or PDA_{60}-pNiPAAm-NH_2/24(39) coatings. (b) Representative microscopy images of fixed and stained myoblast cells adhering to these (i) PDA/24(39), (ii–iv) PDA/pNiPAAm-NH_2/24(39), (v) pNiPAAm-NH_2/24(39), and (vi) PDA_{60}-pNiPAAm-NH_2/24(39) coatings for 24 h (red: phalloidin, blue: DAPI). The scale bar is 25 μm.

was no significant difference between the number of cells per area adhering to the different coatings observed (Figure 8a). However, when visualizing the adhering cells, the morphology for cells adhering to coatings assembled at 24 and 39 °C was different (Figure 8b). While PDA/24 and PDA/39 equally supported myoblast adhesion, an increasing amount of pNiPAAm-NH_2 in the mixed coatings seemed to exhibit smaller, less spread cells, when the coatings were deposited at 39 °C. It is surprising that the cell spreading appeared negatively affected, because pNiPAAm has reported cell adhesive properties above the LCST.[26] This points toward the fact that pNiPAAm-NH_2, when incorporated into the PDA films, has different properties than the pristine coatings. The cells on pNiPAAm-NH_2/39 films were more spread than expected, probably due to the displacement of the polymer by

dx.doi.org/10.1021/la402118u | *Langmuir* 2013, 29, 10213–10222

the proteins in the media, as previously observed by QCM. Further, PDA_{60}-pNiPAAm-NH_2/24 was supporting cell adhesion and spreading to greater extent than PDA_{60}-pNiPAAm-NH_2/39, likely due to the higher amount of deposited pNiPAAm-NH_2 as the top layer in the latter case. These first *in vitro* experiments demonstrate that, by codeposition of PDA with a polymer, the cell response can be affected and probably eventually steered.

CONCLUSIONS

We demonstrate the assembly of mixed films of PDA and pNiPAAm independent of the end group of the latter component. We employed QCM to assess the film assembly and used XPS to analyze the elemental composition of the coatings and confirmed the presence of mixed films consisting of PDA and pNiPAAm. The optical density of the films was affected by the composition as assessed by UV−vis and found to be highest for PDA/39. We visualized the transition from a PDA film to a pNiPAAm-NH_2 film by increasing the amount of pNiPAAm-NH_2 in the mixture. The protein adsorption to these coatings was monitored by QCM, and it was found that increasing amount of pNiPAAm-NH_2 in the mixed films deposited at 39 °C reduced the protein adsorption independent of the protein adsorption temperature. Further, a PDA deposition temperature-dependent L^{zw} adsorption was identified, that is, increasing the PDA assembly temperature led to higher liposome adsorption. Myoblast cells were used to *in vitro* characterize the films. Coatings assembled at 39 °C yielded small and less spread cells compared to the same coating deposited at 24 °C.

Taken together, we combine two prominent candidate polymers for biomedical applications and, by doing so, are broadening the application possibilities for each of it.

ASSOCIATED CONTENT

Supporting Information

Experimental details, turbidity measurements, dissipation changes ΔD of a QCM crystal upon the polymer deposition, the protein and L^{zw} adsorption, frequency changes Δf of a QCM crystal precoated with different ratios of DA/pNiPAAm-NH_2 upon the exposure to L^{zw}, and a table containing the CA measurements and ELM results. This material is available free of charge via the Internet at http://pubs.acs.org.

AUTHOR INFORMATION

Corresponding Author

*M.Z.: E-mail: zmf@dhu.edu.cn. B.S.: Tel: +45 8715 6668; e-mail: bstadler@inano.au.dk

Notes

The authors declare no competing financial interest.

ACKNOWLEDGMENTS

This work was supported by a Sapere Aude Starting Grant from the Danish Council for Independent Research, Technology and Production Sciences, Denmark, and National Natural Science Foundation for Distinguished Young Scholar of China (50925312). We also thank Associate Prof. Rikke L. Meyer (iNANO, Aarhus University, Denmark) for access to the AFM and CLSM, Assist. Prof Alexander N. Zelikin for access to the multiplate reader, and Dr. Joseph Iruthayaraj for help with the ELM measurements.

REFERENCES

(1) Hudalla, G. A.; Murphy, W. L. *Soft Matter* **2011**, *7*, 9561−9571.
(2) Gribova, V.; Auzely-Velty, R.; Picart, C. *Chem. Mater.* **2012**, *24*, 854−869.
(3) Lynge, M. E.; van der Westen, R.; Postma, A.; Stadler, B. *Nanoscale* **2011**, *3*, 4916−4928.
(4) Zelikin, A. N. *ACS Nano* **2010**, *4*, 2494−2509.
(5) Hosta-Rigau, L.; Jensen, B. E. B.; Fjeldsø, K. S.; Postma, A.; Li, G.; Goldie, K. N.; Albericio, F.; Zelikin, A. N.; Städler, B. *Adv. Healthcare Mater.* **2012**, *1*, 791−795.
(6) Lynge, M. E.; Ogaki, R.; Laursen, A. O.; Lovmand, J.; Sutherland, D. S.; Stadler, B. *ACS Appl. Mater. Interfaces* **2011**, *3*, 2142−2147.
(7) Graf, N.; Tanno, A.; Dochter, A.; Rothfuchs, N.; Voros, J.; Zambelli, T. *Soft Matter* **2012**, *8*, 3641−3648.
(8) Smith, R. C.; Riollano, M.; Leung, A.; Hammond, P. T. *Angew. Chem., Int. Ed.* **2009**, *48*, 8974−8977.
(9) Kim, B. S.; Park, S. W.; Hammond, P. T. *ACS Nano* **2008**, *2*, 386−392.
(10) Ball, V.; Del Frari, D.; Michel, M.; Buehler, M. J.; Toniazzo, V.; Singh, M. K.; Gracio, J.; Ruch, D. *BioNanoSci* **2012**, *2*, 16−34.
(11) Lee, H.; Dellatore, S. M.; Miller, W. M.; Messersmith, P. B. *Science* **2007**, *318*, 426−430.
(12) Dreyer, D. R.; Miller, D. J.; Freeman, B. D.; Donald, R. P.; Bielawski, C. W. *Langmuir* **2012**, *28*, 6428−6435.
(13) Hong, S.; Na, Y. S.; Choi, S.; Song, I. T.; Kim, W. Y.; Lee, H. *Adv. Funct. Mater.* **2012**, *22*, 4711−4717.
(14) Vecchia, N. F. D.; Avolio, R.; Alfè, M.; Errico, M. E.; Napolitano, A.; d'Ischia, M. *Adv. Funct. Mater.* **2012**, *23*, 1331−1340.
(15) Jiang, J.; Zhu, L.; Zhu, L.; Zhu, B.; Xu, Y. *Langmuir* **2011**, *27*, 14180−14187.
(16) Xi, Z. Y.; Xu, Y. Y.; Zhu, L. P.; Wang, Y.; Zhu, B. K. *J. Membr. Sci.* **2009**, *327*, 244−253.
(17) Lai, M.; Cai, K. Y.; Zhao, L.; Chen, X. Y.; Hou, Y. H.; Yang, Z. X. *Biomacromolecules* **2011**, *12*, 1097−1105.
(18) Poh, C. K.; Shi, Z. L.; Lim, T. Y.; Neoh, K. G.; Wang, W. *Biomaterials* **2010**, *31*, 1578−1585.
(19) Zhu, L. P.; Jiang, J. H.; Zhu, B. K.; Xu, Y. Y. *Colloids Surf., B: Biointerfaces* **2011**, *86*, 111−118.
(20) Ochs, C. J.; Hong, T.; Such, G. K.; Cui, J.; Postma, A.; Caruso, F. *Chem. Mater.* **2011**, *23*, 3141−3143.
(21) An, J. H.; Huynh, N. T.; Sil Jeon, Y.; Kim, J.-H. *Polym. Int.* **2011**, *60*, 1581−1586.
(22) Zhu, B.; Edmondson, S. *Polymer* **2011**, *52*, 2141−2149.
(23) Tsai, W. B.; Chien, C. Y.; Thissen, H.; Lai, J. Y. *Acta Biomater.* **2011**, *7*, 2518−2525.
(24) Zhang, Y.; Thingholm, B.; Goldie, K. N.; Ogaki, R.; Städler, B. *Langmuir* **2012**, *28*, 17585−17592.
(25) Ramos, J.; Imaz, A.; Forcada, J. *Polym. Chem.* **2012**, *3*, 852−856.
(26) Yang, J.; Yamato, M.; Okano, T. *MRS Bull.* **2005**, *30*, 189−193.
(27) Fukumori, K.; Akiyama, Y.; Kumashiro, Y.; Kobayashi, J.; Yamato, M.; Sakai, K.; Okano, T. *Macromol. Biosci.* **2010**, *10*, 1117−1129.
(28) Xue, C. Y.; Yonet-Tanyeri, N.; Brouette, N.; Sferrazza, M.; Braun, P. V.; Leckband, D. E. *Langmuir* **2011**, *27*, 8810−8818.
(29) Brouette, N.; Xue, C.; Haertlein, M.; Moulin, M.; Fragneto, G.; Leckband, D. E.; Halperin, A.; Sferrazza, M. *Eur. Phys. J.—Spec. Top.* **2012**, *213*, 343−353.
(30) Choi, B. C.; Choi, S.; Leckband, D. E. *Langmuir* **2013**, *29*, 5841−5850.
(31) Quinn, J. F.; Caruso, F. *Langmuir* **2003**, *20*, 20−22.
(32) Burmistrova, A.; Steitz, R.; von Klitzing, R. *ChemPhysChem* **2010**, *11*, 3571−3579.
(33) Serpe, M. J.; Jones, C. D.; Lyon, L. A. *Langmuir* **2003**, *19*, 8759−8764.
(34) Rusu, M.; Kuckling, D.; Möhwald, H.; Schönhoff, M. *J. Colloid Interface Sci.* **2006**, *298*, 124−131.
(35) Tokarev, I.; Minko, S. *Soft Matter* **2009**, *5*, 511−524.
(36) Zhang, Y. J.; Furyk, S.; Sagle, L. B.; Cho, Y.; Bergbreiter, D. E.; Cremer, P. S. *J. Phys. Chem. C* **2007**, *111*, 8916−8924.

(37) Ieong, N. S.; Hasan, M.; Phillips, D. J.; Saaka, Y.; O'Reilly, R. K.; Gibson, M. I. *Polym. Chem.* **2012**, *3*, 794−799.
(38) Li, Z.; Kim, Y.-H.; Min, H. S.; Han, C.-K.; Huh, K. M. *Macromol. Res.* **2010**, *18*, 618−621.
(39) Liu, Z.; Liao, Q. L.; Yang, D. G.; Gao, Y.; Luo, X. J.; Lei, Z. D.; Li, H. M. *Des. Monomers Polym.* **2013**, *16*, 465−474.
(40) Wenzel, R. N. *J. Phys. Chem.* **1949**, *53*, 1466−1467.
(41) Herminghaus, S. *Europhys. Lett.* **2000**, *52*, 165−170.
(42) Rodahl, M.; Hook, F.; Fredriksson, C.; Keller, C. A.; Krozer, A.; Brzezinski, P.; Voinova, M.; Kasemo, B. *Faraday Discuss.* **1997**, *107*, 229−246.
(43) Keller, C. A.; Kasemo, B. *Biophys. J.* **1998**, *75*, 1397−1402.
(44) Masson, M.; Yun, K. S.; Haruyama, T.; Kobatake, E.; Aizawa, M. *Anal. Chem.* **1995**, *67*, 2212−2215.
(45) Reimhult, K.; Petersson, K.; Krozer, A. *Langmuir* **2008**, *24*, 8695−8700.
(46) Bally, M.; Bailey, K.; Sugihara, K.; Grieshaber, D.; Voros, J.; Stadler, B. *Small* **2010**, *6*, 2481−2497.
(47) Malam, Y.; Loizidou, M.; Seifalian, A. M. *Trends Pharmacol. Sci.* **2009**, *30*, 592−599.
(48) Tan, M. L.; Choong, P. F. M.; Dass, C. R. *Peptides* **2010**, *31*, 184−193.
(49) Bernsmann, F.; Frisch, B.; Ringwald, C.; Ball, V. *J. Colloid Interface Sci.* **2010**, *344*, 54−60.